

First-Principles Optical Spectra for F Centers in MgO

Patrick Rinke,^{1,2,3} André Schleife,^{3,4} Emmanouil Kioupakis,^{1,5} Anderson Janotti,¹ Claudia Rödl,^{3,4}
Friedhelm Bechstedt,^{3,4} Matthias Scheffler,^{1,2,3,6} and Chris G. Van de Walle¹

¹Materials Department, University of California, Santa Barbara, California 93106, USA

²Fritz-Haber-Institut der Max-Planck-Gesellschaft, Faradayweg 4–6, 14195 Berlin, Germany

³European Theoretical Spectroscopy Facility (ETSF)

⁴Institut für Festkörperteorie und -optik, Friedrich-Schiller-Universität Jena, Max-Wien-Platz 1, 07743 Jena, Germany

⁵Department of Materials Science and Engineering, University of Michigan, Ann Arbor, Michigan 48109, USA

⁶Chemistry Department, University of California, Santa Barbara, California 93106, USA

(Received 18 November 2011; published 20 March 2012)

The study of the oxygen vacancy (F center) in MgO has been aggravated by the fact that the positively charged and the neutral vacancy (F^+ and F^0 , respectively) absorb at practically identical energies. Here we apply many-body perturbation theory in the G_0W_0 approximation and the Bethe-Salpeter approach to calculate the optical absorption and emission spectrum of the oxygen vacancy in all three charge states. We observe unprecedented agreement between the calculated and the experimental optical absorption spectra for the F^0 and F^+ center. Our calculations reveal that not only the absorption but also the emission spectra of different charge states peak at nearly the same energy, which leads to a reinterpretation of the F center's optical properties.

DOI: 10.1103/PhysRevLett.108.126404

PACS numbers: 71.20.Nr, 71.15.Qe, 71.55.Gs, 78.55.Et

Magnesium oxide (MgO) is a ubiquitous material with applications in a diverse range of areas such as medicine, book preservation, building construction, catalysis, spintronics, electronics, and microelectronics. The anion vacancy in bulk MgO (also called the F or color center) is a—maybe even *the*—classical intrinsic point defect in compound insulators. It is directly or indirectly responsible for many of the material's properties. Still, even after more than five decades of research, the F center [1–9] in MgO remains enigmatic. It is particularly puzzling that the charged and neutral vacancies (F^+ and F^0 , respectively) absorb light at practically identical energies [2,4,6].

Removing an oxygen atom from the MgO lattice results in an s -like defect state (Fig. 1) that can be filled by 2 (F^0), 1 (F^+), or 0 (F^{2+}) electrons [10,11]. Only F^+ is paramagnetic and therefore amenable to detection by electron spin resonance techniques [1–4]. The presence of the diamagnetic F^0 and F^{2+} centers, on the other hand, is typically deduced from optical absorption or luminescence measurements. Unlike in other alkaline earth oxides or alkali halides, this procedure is complicated in MgO by the fact that two optical absorption signals that have been attributed to the oxygen vacancy are very broad and peak nearly at the same energy (4.95 and 5.0 eV [4]). We will demonstrate in this Letter that the F^+ center exhibits a second absorption band at much lower energies that should easily distinguish it from the F^0 center. Moreover, we will show that the

emission energies are also very similar, which leads to a reinterpretation of the optical properties of the oxygen vacancy in MgO.

Thanks to the steadily growing power of modern computing architectures and recent methodological progress, parameter-free calculations are playing an increasingly important role in assigning experimentally observed defect signatures. However, the optical absorption spectrum of the F^0 center in MgO has never been reproduced by first-principles calculations [10,12–16], not even by quantum chemical multireference configuration interaction calculations [15,16]. In this Letter, we demonstrate that state-of-the-art theoretical spectroscopy techniques based on many-body perturbation theory give unprecedented agreement with the experimental spectra if and only if the electron-hole as well as the electron-phonon interactions are included. Defect formation energies are

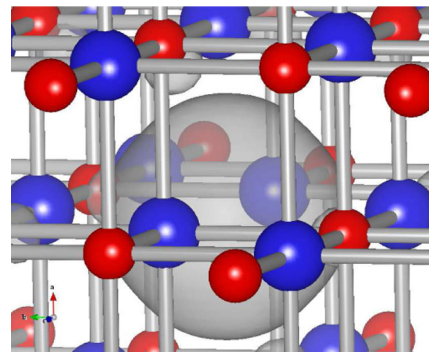


FIG. 1 (color online). Relaxed structure and defect wave function of the F^0 center in MgO. Oxygen atoms are depicted in red (small spheres) and magnesium atoms in blue (large spheres).

Published by the American Physical Society under the terms of the Creative Commons Attribution 3.0 License. Further distribution of this work must maintain attribution to the author(s) and the published article's title, journal citation, and DOI.

calculated based on a recently developed formalism that combines density functional theory (DFT) with many-body perturbation theory in the G_0W_0 approximation [17,18]. The electron-hole interaction is taken into account by solving the Bethe-Salpeter equation (BSE) [19,20]. The electron-phonon interaction is included through the coupling of the optical excitations to local vibrational modes of the defect, which gives rise to a broadening of the absorption spectrum [21,22]. A phonon fine structure is not observed in the experimental optical absorption spectra [4].

All defect structures in this work were relaxed by using the local-density approximation (LDA) and the plane-wave code *S/PHI/NX* [23], unless otherwise stated. Norm-conserving pseudopotentials and a plane-wave cutoff of 70 Ry were used. No nonlinear core corrections were applied. To test the influence of the starting point dependence of G_0W_0 [24,25] for the F center, we also performed calculations with the exact-exchange optimized effective potential approach including LDA correlation (OEPx + cLDA) [24,25] with *S/PHI/NX* by using a plane-wave cutoff of 70 Ry and OEPx + cLDA pseudopotentials [24,25]. In addition, we construct a hybrid scheme as a starting point that mixes 25% exact exchange (Σ_x) with 75% LDA exchange

and correlation (v_{xc}^{LDA}): $v^{LDA0}(\mathbf{r}, \mathbf{r}') = 0.25\Sigma_x(\mathbf{r}, \mathbf{r}') + 0.75v_{xc}^{LDA}(\mathbf{r})$. This new potential, that we term LDA0 due to its similarity with the Perdew-Burke-Ernzerhof hybrid functional (PBE0) [26], is applied perturbatively, i.e., evaluated once with LDA wave functions as input. The G_0W_0 calculations were performed with the *GW* space-time code *GWST* [27] and the BSE calculations with the Vienna *ab initio* simulation package (*VASP*) [20,28,29]. The BSE calculations for the singly occupied defect level of the F^+ center were carried out spin-polarized [30]. Cubic 64-atom bulk and 63-atom defect supercells were used throughout. Total energies of charged defects were corrected by using the scheme by Freysoldt, Neugebauer, and Van de Walle [31]. The correction lies between 0.2 and 0.5 eV for different geometries of the F^+ and 1.6 and 2.2 eV for the F^{2+} center. Quasiparticle energies are converged to 0.1 eV by using a $3 \times 3 \times 3$ Γ -centered \mathbf{k} grid and plane-wave cutoffs of 14 Ha (33 Ha) for the correlation (exchange) part of the *GW* self-energy. Unoccupied states were summed up to 4.5 Ha in the correlation part. Exciton binding energies are converged to 0.05 eV by using Monkhorst-Pack \mathbf{k} -point meshes up to $7 \times 7 \times 7$ and the procedure described in Ref. [20]. All defect calculations were carried out at the LDA lattice constant.

Before we turn to the G_0W_0 corrections for the oxygen vacancy, we will comment on the bulk band gap of MgO. Table I shows that the Kohn-Sham gaps obtained in LDA, OEPx + cLDA, and LDA0 underestimate the experimental gap of 7.78 eV [32] (determined by reflectance spectroscopy). G_0W_0 based on LDA ($G_0W_0@LDA$)

TABLE I. Computed band gaps (in eV) of bulk MgO at the experimental lattice constant of 4.216 Å. The experimental gap is 7.78 eV [32].

	DFT-LDA	DFT-(OEPx + cLDA)	DFT-LDA0
DFT	4.5	6.7	7.0
$G_0W_0@DFT$	7.0	8.1	8.1

also underestimates the gap noticeably, whereas $G_0W_0@(OEPx + cLDA)$ [24,25] and $G_0W_0@LDA0$ yield a much closer value, although they now overestimate.

This overestimation can be rationalized by considering phonon renormalization effects. The coupling to lattice vibrations leads to a temperature-dependent energy change of the electron and hole states. This renormalization is present even at zero temperature because of zero point vibrations. We have calculated this effect by evaluating the electron-phonon self-energy [33,34] for the band-edge states. Approximating the electron-phonon interaction by the Fröhlich expression [35] for intraband transitions, we estimate the band-gap renormalization to be ~ 0.3 eV at zero temperature. This value should be subtracted from any theory that does not automatically include electron-phonon coupling and brings our $G_0W_0@(OEPx + cLDA)$ and $G_0W_0@LDA0$ calculations into good agreement with experiment. We thus apply LDA0 as a starting point for all G_0W_0 defect calculations (since the OEPx + cLDA calculations are computationally too expensive to be applied to the 64- and 63-atom cells used in this work).

The removal of an oxygen atom leaves the MgO lattice relatively unperturbed (see Table II). Once the oxygen vacancy becomes positively charged by removing an electron, the cations are repelled more strongly and move away from the vacancy. The anions, on the other hand, move inward slightly. In the 2+ charge state, the Mg (O) atoms move out (in) further.

$G_0W_0@LDA0$ calculations were then performed for the neutral and 2+ charge states of the oxygen vacancy for each of the three geometries (0, +, and 2+). The energy of the defect states is determined by averaging over the points of a $4 \times 4 \times 4$ \mathbf{k} grid off-centered by (0.5, 0.5, 0.5). For computational convenience, we calculate the electron

TABLE II. Displacement (in angstroms) of the nearest-neighbor Mg and next-nearest-neighbor O atoms computed in LDA. Positive (negative) numbers denote outward (inward) displacements with respect to the MgO lattice positions. F^0 , F^+ , and F^{2+} indicate the three different charge states, whereas $F^0 + h$, $F^+ + e$, and $F^{2+} + e$ refer to the geometry obtained from a constrained-LDA calculation including an extra hole (h) in the valence or an electron (e) in the conduction band.

	F^0	F^+	F^{2+}	$F^0 + h$	$F^+ + e$	$F^{2+} + e$
Mg	0.012	0.090	0.162	0.007	0.082	0.155
O	0.008	-0.027	-0.066	0.010	-0.022	-0.064

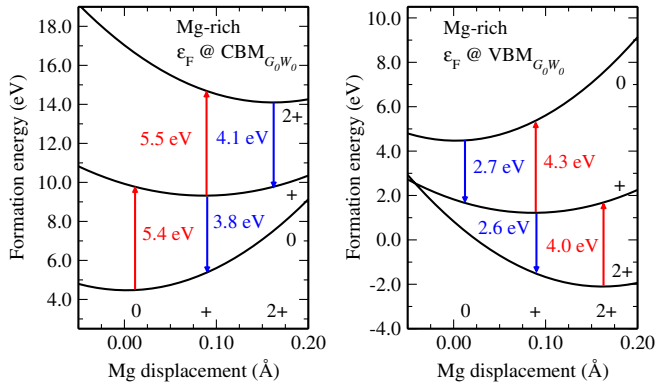


FIG. 2 (color online). Configuration coordinate diagram: The G_0W_0 @LDA0-corrected formation energies in the three different charge states are plotted as a function of the Mg displacement. The lines are a guide to the eye and have been obtained by fitting parabolas to the three data points of each curve. In the left panel the Fermi level is aligned with the conduction-band minimum (CBM) and in the right with the valence-band maximum (VBM). Red (blue) arrows mark absorption (emission) processes.

affinity of 1+ states by their inverse process, the electron removal from the neutral state, since no spin polarization or partially filled defect states are encountered then [18,36]. We add these electron affinities to the LDA formation energies of the respective 2+ states to build up the GW -correction scheme [17,18]. We can then draw the configuration coordinate diagrams presented in Fig. 2.

To first approximation we can view the absorption process of an F^0 center as creating an F^+ center plus an electron in the conduction band. The absorption energies can then be read off Fig. 2 and are summarized in Table III. Values obtained from LDA are also included in Table III and not unexpectedly considerably underestimate the absorption energies. G_0W_0 @LDA0 improves on LDA but now overestimates the absorption energy, because the interaction between the electron in the conduction band and the remaining hole on the defect has not yet been taken into account.

We do this by solving the BSE by using an efficient scheme to converge the exciton binding energies [20]. The resulting values, which we subtract from the G_0W_0 @LDA0 transition energies to obtain the absorption

TABLE III. Computed optical absorption energies (in eV) for the F^0 and F^+ center compared to the experimental values from Ref. [6].

	F^0	F^+
LDA	3.00	4.10
G_0W_0 @LDA0 corrected transition	5.40	5.48
BSE exciton binding energy	0.45	0.56
G_0W_0 @LDA0 – BSE	4.95	4.92
Experiment	5.00	4.95

energies for the F^0 and F^+ center, are also listed in Table III. To estimate the peak broadening we perform constrained-LDA calculations during which the defect is allowed to relax subject to the constraint that for the F^0 center an electron is held in the conduction band, whereas the hole remains on the defect ($F^+ + e$ in Table II). The same constrained calculation is performed for the F^+ center ($F^{2+} + e$), while $F + h$ denotes the scenario of a hole in the valence band that has been created by promoting an electron from the valence band into the F^+ center. As Table II demonstrates, the resulting geometries are close to those of the corresponding charge states without the extra charge in the conduction or valence band. We then linearly interpolate the relaxed structures in the ground and the constrained state by using five intermediate structures and calculate the constrained-LDA energy for each. The points fall on a parabola from which we extract the vibrational energies and Huang-Rhys factors [37]. Those combined (and including a broadening of 80 meV for each vibrational state) give the vibrationally broadened optical spectra shown in Fig. 3. These computed spectra are in unprecedented agreement with experiment.

The peak at lower energies in the theoretical spectrum in Fig. 3 is associated to the F^+ center, which, since it holds only one electron, offers two spin channels. The electron in the occupied state can be excited out of the F^+ center in the optical absorption event (peak at 4.92 eV), whereas the empty spin state can be filled by an excitation of an electron from the valence band (peak at 3.6 eV). Consequently, we see two peaks in our BSE calculations for the F^+ center. Similar absorption processes have been observed for other defects [22] but have, with the exception of Rosenblatt *et al.* [5], never been discussed for the oxygen vacancy in MgO. We see no reason why such a process should not occur and argue that such a two-peak structure would be a much more unambiguous fingerprint for the F^+ center than trying to distinguish its peak at 4.95 eV from the one of the F^0 center at 5.0 eV.

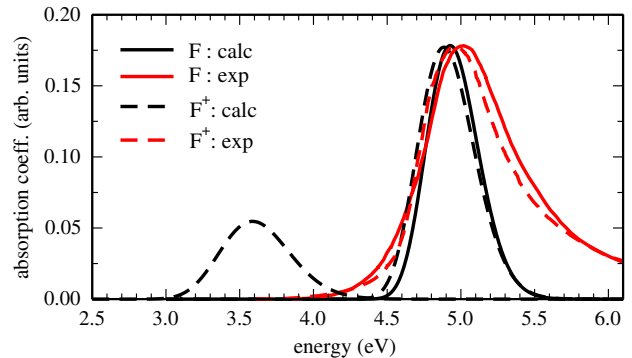


FIG. 3 (color online). Calculated and experimental [4] optical absorption spectra for the F^0 and F^+ center. The peak at lower energies corresponds to the absorption of an electron from the valence band into the F^+ center. For the F^+ center the relative peak heights are taken from the BSE calculations.

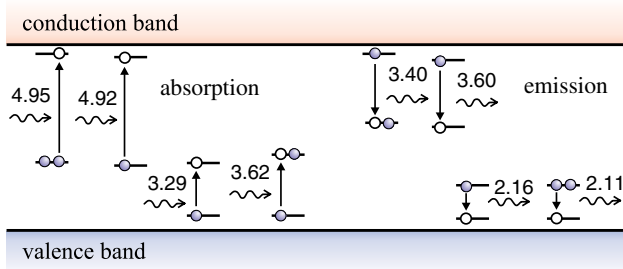


FIG. 4 (color online). The four possible absorption (left) and emission (right) processes of the oxygen vacancy in MgO. Filled circles denote electrons and empty circles holes.

To complete the picture, we now briefly turn to the emission spectra of the oxygen vacancy. Two distinct emission signals have been observed experimentally at 2.3–2.4 and at 3.1–3.2 eV [3–6,8,9]. They have been ascribed to the F^+ and F^0 center, respectively, and have been used as a way to distinguish these two charge states. However, considering that both centers absorb at nearly the same energy, it would be surprising if they would not also emit at nearly the same energy. In our calculations this is in fact the case, as Fig. 4 illustrates: F^0 -center emission would peak at 3.4 eV, whereas F^+ -center emission lies at 3.6 eV (we have obtained the emission energies analogous to the absorption energies, by subtracting the corresponding exciton binding energies from the blue transitions in Fig. 2). These numbers are not as close to the experimental 3.1–3.2 eV as we observed for absorption but fall well into the very broad experimental peak and unambiguously rule out emission around 2.3–2.4 eV. Emission at those energies occurs when electrons in F^0 and F^+ centers recombine with holes in the valence band (see Fig. 4). Holes are created during the photobleaching process [continuous irradiation with intense UV light (~ 5 eV)].

This leads us to a simple argument for why the original emission-peak assignment might have been made. Rosenblatt *et al.* argue that the photoexcitation or photobleaching processes ionize the centers; i.e., the excitonic state is close enough to the conduction-band edge that the electron escapes and becomes a free carrier. This implies that recombination does not necessarily occur at the site where the electron-hole pair has been created. The free electrons are then naturally attracted by the positively charged F^+ or F^{2+} centers and predominantly recombine there (emission at 3.1–3.2 eV), irrespective of whether the two different charge states have been created by bleaching or were already present. This would explain the observed correlation between the 3.1–3.2 eV signal and the F^+ center density (no free-electron recombination can occur at F^0 centers). The opposite is true for free holes in the valence band. They are repelled by the positive F^+ center and preferably recombine at an F^0 -center site (emission at 2.3–2.4 eV), which explains the correlation between the 2.3–2.4 eV signal and the F^0 -center density.

In conclusion, we have reported unprecedented agreement between optical absorption measurements and many-body theory calculations for the F^0 and F^+ center in MgO, which can be achieved only when quasiparticle effects as well as the electron-hole and electron-phonon interactions are explicitly included. We suggest a two-peak structure in the optical absorption of the F^+ center as an easier way to identify this charge state of the oxygen vacancy and offer a reinterpretation of the assignments of emission peaks to different charge states of the F center in MgO.

We gratefully acknowledge fruitful discussions with K. Delaney, P. Allen, and M. Stavola. This work was supported by the NSF MRSEC Program (DMR05-20415), the EU's Seventh Framework Program through the European Theoretical Spectroscopy Facility e-Infrastructure grant (No. 211956), and the DFG (Be 1346/20-1). P. R. acknowledges the DFG, the UCSB-MPG Exchange, and the NSF-IMI Program (DMR04-09848). A. S. thanks the Carl-Zeiss-Stiftung and Heptagon for support.

-
- [1] J. E. Wertz, P. Auzins, R. A. Weeks, and R. H. Silsbee, *Phys. Rev.* **107**, 1535 (1957).
 - [2] J. C. Kemp, J. C. Cheng, E. H. Izen, and F. A. Modine, *Phys. Rev.* **179**, 818 (1969).
 - [3] Y. Chen, J. L. Kolopus, and W. A. Sibley, *Phys. Rev.* **186**, 865 (1969).
 - [4] L. A. Kappers, R. L. Kroes, and E. B. Hensley, *Phys. Rev. B* **1**, 4151 (1970).
 - [5] G. H. Rosenblatt, M. W. Rowe, G. P. Williams, R. T. Williams, and Y. Chen, *Phys. Rev. B* **39**, 10309 (1989).
 - [6] Y. Chen, V. M. Orera, R. Gonzalez, R. T. Williams, G. P. Williams, G. H. Rosenblatt, and G. J. Pogatschnik, *Phys. Rev. B* **42**, 1410 (1990).
 - [7] M. Sterrer, E. Fischbach, T. Risse, and H.-J. Freund, *Phys. Rev. Lett.* **94**, 186101 (2005).
 - [8] A. Lushchik, T. Kärner, C. Lushchik, E. Vasil'chenko, S. Dolgov, V. Issahanyan, and P. Liblik, *Phys. Status Solidi C* **4**, 1084 (2007).
 - [9] E. Feldbach, R. Jaaniso, M. Kodu, V. Denks, A. Kasikov, P. Liblik, A. Maaros, H. Mändar, and M. Kirm, *J. Mater. Sci. Mater. Electron.* **20**, 321 (2008).
 - [10] B. M. Klein, W. E. Pickett, L. L. Boyer, and R. Zeller, *Phys. Rev. B* **35**, 5802 (1987).
 - [11] A. Janotti and C. G. Van de Walle, *Nature Mater.* **6**, 44 (2007).
 - [12] R. Pandey and J. M. Vail, *J. Phys. Condens. Matter* **1**, 2801 (1989).
 - [13] A. De Vita, M. J. Gillan, J. S. Lin, M. C. Payne, I. Štich, and L. J. Clarke, *Phys. Rev. B* **46**, 12964 (1992).
 - [14] E. Scorza, U. Birkenheuer, and C. Pisani, *J. Chem. Phys.* **107**, 9645 (1997).
 - [15] F. Illas and G. Pacchioni, *J. Chem. Phys.* **108**, 7835 (1998).
 - [16] C. Sousa and F. Illas, *J. Chem. Phys.* **115**, 1435 (2001).
 - [17] M. Hedström, A. Schindlmayr, G. Schwarz, and M. Scheffler, *Phys. Rev. Lett.* **97**, 226401 (2006).

- [18] P. Rinke, A. Janotti, M. Scheffler, and C. G. Van de Walle, *Phys. Rev. Lett.* **102**, 026402 (2009).
- [19] G. Onida, L. Reining, and A. Rubio, *Rev. Mod. Phys.* **74**, 601 (2002).
- [20] F. Fuchs, C. Rödl, A. Schleife, and F. Bechstedt, *Phys. Rev. B* **78**, 085103 (2008).
- [21] Y. Ma and M. Rohlfing, *Phys. Rev. B* **77**, 115118 (2008).
- [22] M. Bockstedte, A. Marini, O. Pankratov, and A. Rubio, *Phys. Rev. Lett.* **105**, 026401 (2010).
- [23] S. Boeck, C. Freysoldt, A. Dick, L. Ismer, and J. Neugebauer, *Comput. Phys. Commun.* **182**, 543 (2011).
- [24] P. Rinke, A. Qteish, J. Neugebauer, C. Freysoldt, and M. Scheffler, *New J. Phys.* **7**, 126 (2005).
- [25] P. Rinke, A. Qteish, J. Neugebauer, and M. Scheffler, *Phys. Status Solidi B* **245**, 929 (2008).
- [26] J. P. Perdew, K. Burke, and M. Ernzerhof, *Phys. Rev. Lett.* **77**, 3865 (1996); *J. Chem. Phys.* **105**, 9982 (1996).
- [27] M. M. Rieger *et al.*, *Comput. Phys. Commun.* **117**, 211 (1999); L. Steinbeck *et al.*, *Comput. Phys. Commun.* **125**, 105 (2000); C. Freysoldt *et al.*, *Comput. Phys. Commun.* **176**, 1 (2007).
- [28] G. Kresse and J. Furthmüller, *Phys. Rev. B* **54**, 11 169 (1996).
- [29] G. Kresse and J. Furthmüller, *Comput. Mater. Sci.* **6**, 15 (1996).
- [30] C. Rödl, F. Fuchs, J. Furthmüller, and F. Bechstedt, *Phys. Rev. B* **77**, 184408 (2008).
- [31] C. Freysoldt, J. Neugebauer, and C. G. Van de Walle, *Phys. Rev. Lett.* **102**, 016402 (2009).
- [32] R. C. Whited and W. C. Walker, *Phys. Rev. Lett.* **22**, 1428 (1969).
- [33] P. B. Allen and M. Cardona, *Phys. Rev. B* **23**, 1495 (1981).
- [34] C.-H. Park, F. Giustino, M. L. Cohen, and S. G. Louie, *Phys. Rev. Lett.* **99**, 086804 (2007).
- [35] O. Madelung, *Introduction to Solid-State Theory* (Springer-Verlag, Berlin, 1978).
- [36] M. Giantomassi, M. Stankovski, R. Shaltaf, M. Grüning, F. Bruneval, P. Rinke, and G.-M. Rignanese, *Phys. Status Solidi B* **248**, 275 (2011).
- [37] G. Davies, in *Identification of Defects in Semiconductors*, edited by M. Stavola (Academic, New York, 1998), Vol. 51b.